Investigation on Compressible Bi-Convex Corner Flows

K.M. Chung[1], K.C. Chang[2] and P.H. Chang[2]

[1] Aerospace Science and Technology Research Center; [2]Institute of Aeronautics and Astronautics, National Cheng Kung University, Tainan 711, Taiwan, Republic of China

Abstract

This study addressed the shock-wave and turbulent boundary layer interactions of bi-convex corner flows. The experimental data were conducted at freestream Mach number of 0.64, 0.70, 0.83 and 0.89. A row of flush-mounted, high frequency pressure transducer was used to measure the mean and fluctuating pressures. In comparison with a single convex corner flows, a bi-convex corner tends to alleviate shock induced boundary layer separation and the location of peak pressure fluctuations moves downstream. The surface pressure fluctuation and local Mach number could be scaled with a similarity parameter β. In addition, the hypersonic similarity was also used to correlate the experimental data. Generally, the correlation is reasonably good.

Introduction

Applications of variable camber wings have been explored and studied extensively since 1980s [1]. Employing variable leading- and/or trailing-edge camber or mission-optimized local or global shapes can result in appreciable drag reductions for a military aircraft and a long-range civil transport aircraft [2-6]. As shown in Fig. 1, a variable camber wing leads to an optimization of the L/D ratio at a given angle of attack. However, flap deflections may lead to boundary layer separation at transonic flight conditions. Besides, with rapid shape variation, the damping of the dynamic aeroelastic phenomena, vibrations and noise might be augmented [8-10]. In order to avoid the drawbacks, the trailing-edge devices of a wing evolve from plain flaps to Fowler flaps with single, double, and even triple slots.

As an incoming flow, whether it is laminar or turbulent, accelerates from subsonic to supersonic speed over an expansion corner, the flow pattern would be changed significantly from that expected by an inviscid theory. The shock wave would occur due to inviscid-viscous interactions and might result in boundary layer separation. Generally, the critical Mach number is about 1.32, which is associated with the adverse pressure gradient across the shock wave. From the previous studies [11], it is known that the peak Mach number of a deflected flap (or a single convex corner) in compressible flows could be scaled with freestream Mach number and the deflection angle. Later studies [12] provided more information on the fluctuating wall pressure in the interaction regions of two-dimensional convex corner flowfields. These results indicate that a similarity parameter, $\beta = M^2\eta/\sqrt{1-M^2}$, which combined with the variable change of hodograph equation and Prandtl – Glauert rule, could be used to characterize the flow characteristics. To simulate a flow over multiple slots, bi-convex corner models were used in this study. β is also used to characterize the flow development. Besides, the correlation of mean pressure coefficient and hypersonic similarity parameter $M\eta$ was addressed

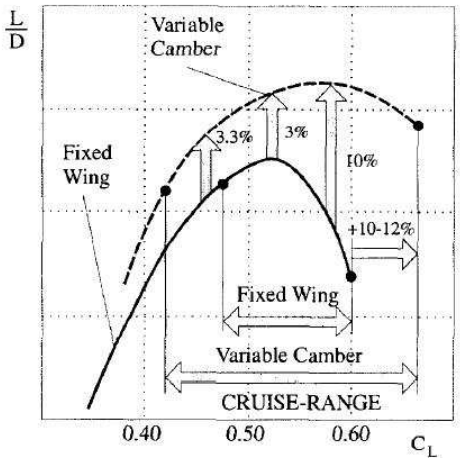

Fig. 1 Variable camber effect on L/D [6, 7]

Experimental set-up

The experiments were carried out in the Aerospace Science and Technology Research Center/ National Cheng Kung University (ASTRC/NCKU) blowdown transonic wind tunnel. This tunnel has a constant area test section that measures 600 × 600 mm in cross section and 1500 mm in length. Major components of the facility comprise compressors, air dryers, a cooling water system, and three air storage tanks. The incoming boundary layer along a flat plate made a natural transition to turbulence. So, the boundary layer upstream of the bi-convex corner is fully turbulent [11]. The freestream Mach numbers were 0.64, 0.70, 0.83 and 0.89±0.01, and the unit Reynolds number ranged from 12.1 to 24.1 million per meter. Stagnation pressure is kept constant at 172±0.5 kPa and stagnation temperature is of room temperature.

A bi-convex corner model was made of a flat plate, an instrumentation plate and a single-foot support placed fixed on the bottom wall of the test section, as shown in Fig. 2. The instrumentation plate was 150 (width) × 170 (length) mm. The initial deflection angles η_1 were 5° or 7°, and the second deflection angle η_2 ranged from 6° to 12°, as shown in Tab. 1. Thus, the combined convex-corner angle η (=η_1+η_2) ranged from 13° to 17°. Note that the side fences were used at both sides to prevent crossflow, in which the flows were essentially two-dimensional with minor three-dimensional perturbations [11].

The NEFF 620 System and the NI-PXI recorders were used as the data acquisition systems. The test conditions of wind tunnel were recorded by the NEFF 620 System, whereas the NI-PXI recorders were used for the surface pressure measurements with the flush-mounted Kulite pressure transducers (XCS-093-25A, B screen) along the bi-convex models. The pressure transducers have a nominal outer diameter of 2.36 mm and a pressure-sensitive diaphragm 0.97 mm in diameter. The natural frequency was quoted by the manufacturer to be close to 200 kHz. A Topward Electronic System Model 6102 power supply at 15.0 V was used to power all pressure transducers. External amplifiers (Ecreon Model E713), in which the roll-off frequency is about 140 kHz, were also used to improve the signal-to-noise ratio. All input channels were triggered simultaneously. Furthermore, the typical sampling rate in the present study is 200 ksamples/s (or 5μs). In all tests, statistical analysis was obtained by ensemble averaging time series made of 32 blocks of 4096 points. The uncertainty of experimental data was estimated to be 0.43 and 0.13% for the mean surface pressure coefficient C_p and the fluctuating pressure coefficient $C_{\sigma p}$, respectively.

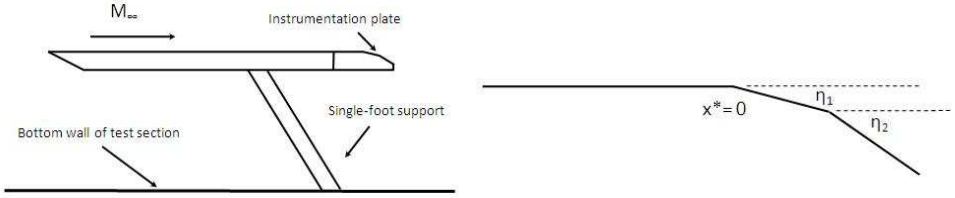

Fig. 2 Test configuration

The angle of bi-convex corner

Combined convex-corner angle η (= η_1+η_2)	The initial deflection angles η_1	The second deflection angle η_2
η = 13°	5°	8°
	7°	6°
η = 15°	5°	10°
	7°	8°
η = 17°	5°	12°
	7°	10°

Result and discussion

Wall-Pressure Distributions. The time-history plots of the fluctuating wall pressure (for the 15 deg model at M = 0.83) were shown in Fig. 3. It can be seen that the signals with η_1 and η_2 are 7° and 8°, respectively, were highly intermittent and appeared to jump back and forth between two levels, which the undisturbed level indicated by P_1 and the " high" level marked P_2. It is plausible that P_2 is the level measured when the "foot" of the shock wave was upstream of the transducer and

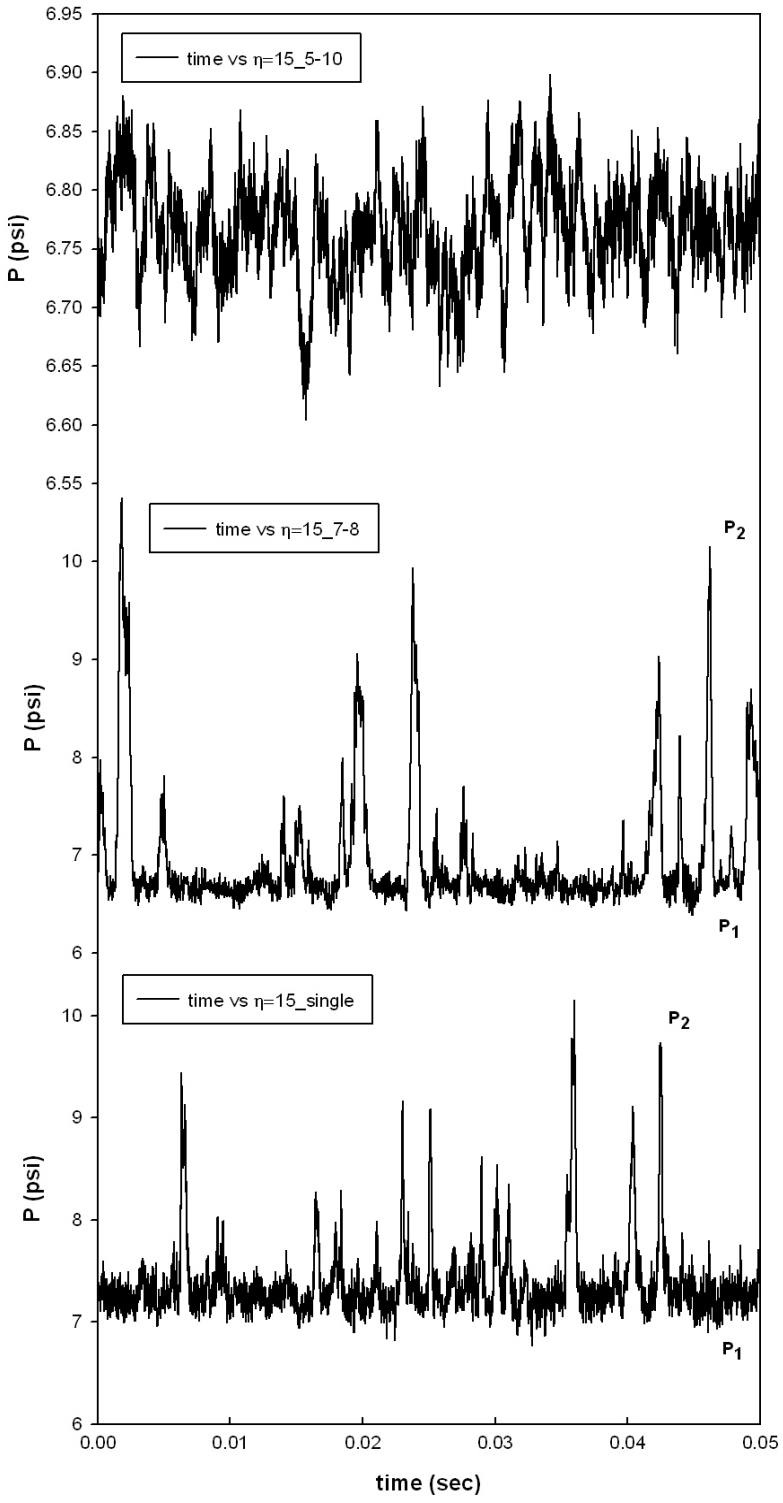

Fig. 3 Time-history plots of the fluctuation wall pressure

vice versa, while P_1 was measured when the shock moved toward downstream of the transducer. Besides, a number of spikes were also seen in this figure; these were probably measured when the shock foot just met the location of the transducer. On the other hand, the time-history signals in 5°–10° bi-convex corner flow did not appear the obvious pressure peaks. With this view, a milder two-stage flap could reduce the percentage of the occurrence of shock wave and weaken the strength of shock. As a result, one might expect that a milder two-stage flap would avoid shock induced boundary layer separation.

Fluctuating Pressure Distribution. Figure 4 showed the distributions of normalized surface pressure fluctuation at different type of combinations for 15 deg model (M = 0.83), and these results compared with that of the single flap data. It can be seen that the pressure fluctuations were roughly constant in the upstream and downstream interaction regions. On the other hand, it was worth pointing out that the maximum pressure fluctuations in the vicinity of corner were relative lower over a bi-convex corner. These results indicated that the bi-convex corner only had an influence on the local flowfield within the corner region. It is interesting to note that peak pressure fluctuations dropped with increasing η_1 of convex-corner. As can be seen in Fig. 4, the peak pressure fluctuation had a difference of 30% between the single corner and the 5°–8° bi-convex corner. It is considered that the boundary-layer thickness might become thinner than that of a single convex corner. Besides, the position of peak pressure fluctuation moved toward downstream with increasing η_1.

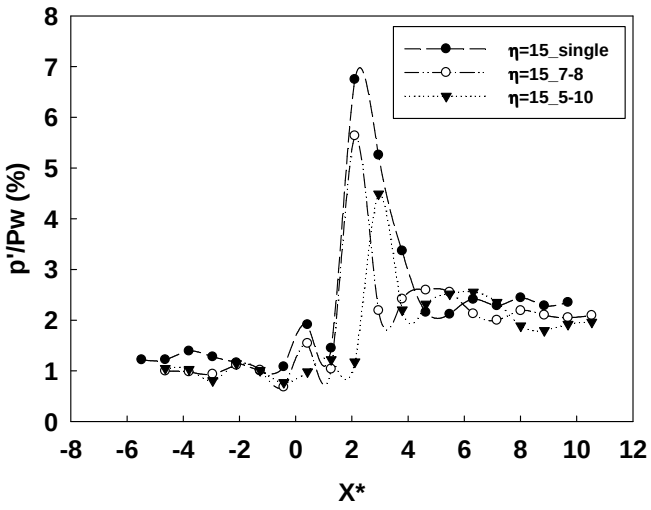

Fig. 4 Longitudinal distribution of rms pressure fluctuation

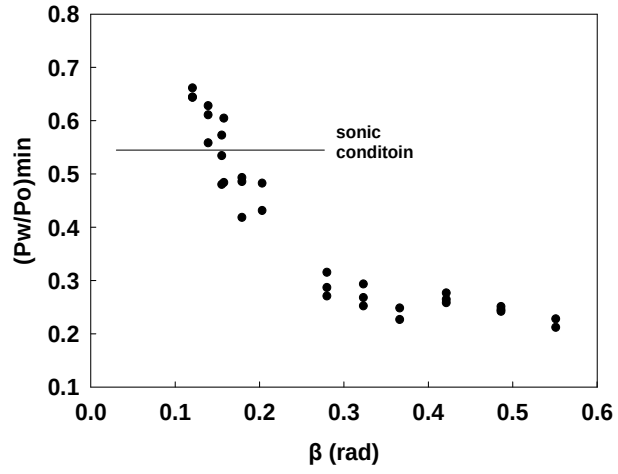

Fig. 5 Surface pressure distribution

Similarity Parameter. The mean surface pressure coefficient (P_w/P_o) and local peak Mach number were plotted against β, as shown in Fig. 5. Note that P_w/P_o = 0.528 corresponds to the sonic condition. For β< 0.19, the flowfield was a typical subsonic expansion. It can be seen that both mean surface pressure coefficient and local Mach number can be scaled with β. Apparently, the (P_w/P_o) may be roughly grouped into two regimes. One represented that $(P_w/P_o)_{min}$ decreased linearly with increasing β in the range of 0.12 and 0.21. As β> 0.35, there was an approach to an asymptotic value of 0.2–0.3, which would refer to "free interaction" [13].

The concept of hypersonic similarity Mη (or *K*) was proposed first developed by Hsien [14] in 1946, which is based on small-disturbance equations. Previous studies on hypersonic flows had demonstrated that C_p/η^2 is a function of specific heat ratio, γ and *K* only. The relation between C_p and β could be rewrote in term of C_p/η^2 and $M^2/\eta\sqrt{(1-M^2)}$ [alternative β i.e. β′]. The denominator of β′ was supersonic-hypersonic similarity, which was proposed by Van Dyke [15]. For compressible con-

vex-core flows, the current data, as shown in Fig. 6, were scaled using Cp/η^2 and β'. It can be seen that the Cp/η^2 decreased linearly with increasing β'. However, the data of bi-convex flows exhibit relatively little scatter at smaller η but diverge thereafter.

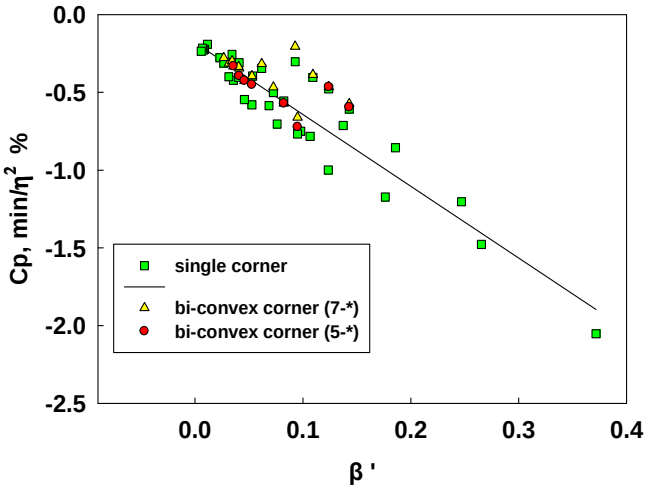

Fig. 6 Pressure coefficient distribution

Conclusion

In this experimental investigation, the flow over bi-convex corners was examined. There was a delay of transition from subsonic to supersonic flow regimes. It is also found that the bi-convex corner could alleviate shock-induced boundary layer separation. The location of the peak pressure fluctuations moved downstream. At larger β, the mean surface pressure coefficient and local peak Mach number approached asymptotic values, which was governed by the concept of free interaction. Both β and K were also used to correlate the experimental data. Generally, the results showed that the correlations are reasonably good.

REFERENCES

1. **Szodruch J., Hilbig R.** Variable wing camber for transport aircraft // Prog. Aerospace Sci. 1988. Vol. 25. P. 297–328.
2. **Ashill P.R., Fulker J.L., Simmons M.J.** Simulated Active Control of Shock Waves in Experiments on Aerofoil Models // Prog. ICEFM, Turin, July 1994.
3. **Martins A.L., Catalano F.M.** Viscous Drag Optimization for a Transport Aircraft Mission Adaptive Wing // Prog. 21st ICAS Congress, Melbourne, Australia, A98-31499, 1998.
4. **Siclari M.J., Nostrand, W. van, Austin, F.** The Design of Transonic Airfoil Sections of an Adaptive Wing Concept Using a Stochastic Optimization Method, AIAA 34th Aerospace Science Meeting & Exhibit, Reno, NV, Paper AIAA–96–0329, 1996.
5. **Smith S.B., Nelson D.W.** Determination of the aerodynamic characteristic of the mission adaptive wing // J. Aircraft. 1990. Vol. 27, No. 11. P. 950–958.
6. **Szodruch J.** The influence of Camber Variation on the Aerodynamics of Civil Transport Aircraft, AIAA Aerospace Science Meeting, Reno, NV, Paper AIAA-85-0353, 1985.
7. **Hilbig H., Wagner H.** Variable wing camber control for civil transport aircraft // Prog. ICAS–84–5.2.1, P. 107–112, Toulouse, 1984.
8. **Büter A., Breitbach E.** Adaptive blade twist – calculations and experimental results // Aerosp. Sci. Technol. 2000. Vol. 4. P. 309–319.
9. **Lin C.Y., Crawley E.F., Heeg J.** Open- and closed-loop results of a strain-actuated active aeroelastic wing // J. Aircraft. 1996. Vol. 33. P. 987–994.
10. **Wilkie W.K., Belvin W.K., Park K.C.** Aeroelastic analysis of helicopter rotor blades incorporating anisotropic piezoelectric twist actuation. NASA Langley Research Center – Aeroelasticity Branch, 1997.
11. **Chung K.M.** Transonic of subsonic and transonic expansion-corner flows // J. Aircraft. 2000. Vol. 37, No. 6. P. 1079–1082.
12. **Chung K.M., Chang P.H., Chang K.C.** Flow similarity in compressible convex-corner flows // AIAA J., 2012, Vol. 50 (4)
13. **Chapman D.R., Kuehn D.M., Larson H.K.** Investigation of separated flows in supersonic and subsonic stream with emphasis on the effect of transonic: NACA TN 3869, 1957.
14. **Tsien H. S.** Similarity laws of hypersonic flows // J. Mathematics and Physics. 1946. Vol. 25, P. 247-251.
15. **Van Dyke M. D.** The combined supersonic and hypersonic similarity rule // J. Aeronautical Science. 1951. Vol. 18, No. 7. P. 499–500.